Pak. J. Agri. Sci., Vol. 56(X), xxx-xxx; 2019
ISSN (Print) 0552-9034, ISSN (Online) 2076-0906
DOI: 10.21162/PAKJAS/19.7750
http://www.pakjas.com.pk

CONTRIBUTION TO SPRAYING NOZZLE STUDY: A COMPARATIVE INVESTIGATION OF IMAGING AND SIMULATION APPROACHES

Muhammad Nadeem[1,2], Tri Nguyen-Quang[2*], Claver Diallo[1], Uday Venkatadri[1] and Peter Havard[2]

[1]Department of Industrial Engineering, Dalhousie University, PO BOX 15000, Halifax, NS, B3H 4R2, Canada;
[2]Department of Engineering, Faculty of Agriculture, Dalhousie University, 39 Cox Road, Truro, Nova Scotia, B2N 5E3, Canada.
[*]Corresponding author's e-mail: tri.nguyen-quang@dal.ca

Application of agrochemicals on crops is important for plants protection. Multiple factors influence the application of agrochemicals on plants such as climatic conditions, crop characteristics and spraying system design. There is a need for reliable methods to investigate these properties more precisely with low cost and in reasonable time. In the present study, the velocity distribution of an extended flat fan nozzle is investigated to determine the weak jet areas, which have high risks of droplet drift. Two methods are used and compared: the Particle Image Velocimetry (PIV) method used as an experimental approach versus a Computational Fluid Dynamics (CFD) with volume of fluid (VOF) integrating k-epsilon model as a simulation approach. The nozzle was operated at eight different pressures on a custom-made nozzle operating prototype while ANSYS 16 Fluent software was employed for the simulation approach. The obtained findings showed three significant results. First, the spray sheet (jet) has maximum velocity in its center. Second, the particles present in the central region of spray sheet have maximum kinetic energy and this region has the ability to hit the right target on the plant surface, while liquid particles present in the surroundings of this central area have less velocity with minimum kinetic energy and have maximum chances to be off-target during spraying. These particles can move away from the targeted surfaces easily even with very low wind velocity. Third, the study also showed that PIV and CFD simulation methods were in agreement and both showed reliable ways to measure the jet velocity and plot the velocity distribution under the sprayer nozzle. The applications of these findings are also discussed.

Keywords: CFD, Jet velocity, Numerical simulation, Particle Image Velocimetry (PIV), Spray uniformity, Turbulence flow

INTRODUCTION

Application of agrochemicals on crops is important for plants protection. The quality of agrochemicals plays a vital role in the application of agrochemicals using different types of sprayer nozzles. The sprayer efficiency can be maximized by selecting the appropriate nozzle pressure combination which increases the deposition rate of agrochemicals on plant surface (Smith *et al.,* 2000), reduces the runoff of agrochemicals on soils (Derksen *et al.,* 2008), and reduces the drift prone hazards (Nuyttens *et al.,* 2007; Yarpuz and Bozdogan, 2009). The efficiency of agrochemicals application depends on characteristics of the spray such as droplet size, operating pressure, droplet velocity, entering air characteristics, and volume distribution characteristics (Nuyttens *et al.,* 2009). In this study, we will discuss the velocity characteristic behavior of sprayer nozzle under different pressures.

Droplet size, pressure and velocity are the most important factors during the application of agrochemicals. Studies are available on droplet distribution of sprayer pattern (Bird *et al.,* 1996; Carlsen *et al.,* 2006; Ozkan *et al.,* 1997; Nuyttens *et al.,* 2007; Piggott and Matthews, 1999; Etheridge *et al.,* 1999). These studies showed that droplet distribution throughout the spray sheet is not homogenous and the droplet distribution depends upon the position of droplet within the spray sheet.

Droplets after leaving the nozzle are three-dimensional (Farooq *et al.,* 2001). The authors reported that the increase in pressure of spray not only decreases the droplet size but also increases the velocity of spray when leaving the nozzle. In other words, increasing the pressure produce more fine spray particles which have more tendency for drift but at the same time high pressure increase the velocity of droplets (Ozkan, 1998). According to Miller and Ellis (1997), after a certain limit of pressure the drift of spray decreases due to the dominance of droplet velocity.

Nuyttens *et al.* (2009) worked on droplet and velocity characteristics of agricultural sprayers. They evaluated 13 different nozzles-pressure combinations by using Phase Doppler Particle Analyzer (PDPA) and concluded that the smaller droplets had less velocity and larger droplets had high velocity. The velocity of bigger droplets (>400 µm) varies from 4.5-8.5 m/s but depending upon the nozzle type and size when operated at 3.0 bar pressure. In the same way, velocity

of droplets less than 400 µm decreases consistently with decrease in droplet size. This velocity varies from 0.5-2 m/s but it also depends upon nozzle type, pressure, orifice shape and size (Nuyttens *et al.,* 2009).

The study of high-pressure liquid flowing from one medium to another is still a difficult theme in modeling. The development of droplets after the fluid comes out of the nozzle into air is still an interesting topic to understand the instability of jet. For example, in our case study, water is coming out of a nozzle into a lighter medium by pressure. There are many studies underlined the phenomenon of liquid jet entering in liquid medium. However, less works have been reported to understand the jet phenomenon from nozzle-liquid medium going to the air. At low Reynolds number, the jet of water coming in lighter medium brakes up due to hydrodynamic instability and surface tension is a major contributor towards this instability (Sinha *et al.,* 2015). Behavior of jet is wavy at high Reynolds number due to the induction of aerodynamic effects. Reynolds number, the ratio of inertial force to viscous force, is a dimensionless quantity used to 'quantify' the flow patterns in different flow conditions. Fundamental fluid mechanics showed very well that laminar flow occurs at low Reynolds number while turbulence at high Reynolds number, including in the jet flow (Sinha *et al.,* 2015). Taylor and Hoyt (1977), and Chaudhary and Maxworthy (1980) conducted experiments on water jet behavior and concluded that density also had significant effect on the characteristics of water jet behavior. Lin and Reitz (1998) studied injection of water jet in gas and reported the behavior of jet in four different regimes. These regimes are identified based on viscosity, density, gravity and surface tension. The four regimes are classified as 1) the Rayleigh regime, where jet diameter < droplet diameter; 2) the 1st wind induced regime, where jet diameter = droplet diameter; 3) the 2nd wind regime, where jet diameter > droplet diameter; and 4) the atomization regime, where droplet diameter is negligible as compared to jet diameter (Homma *et al.,* 2006). The behavior of droplet changes from 2D to 3D when injected from high density to another low-density medium (Homma *et al.,* 2006). In the case of water jet coming out from nozzle like in our case study, the atomization regime occurs given that the average droplet diameter (288 µm) (ASABE, 2010) is negligible when compared to the jet diameter (1500 µm) TEEJET 8003 (extended range flat fan). The characteristics of such fluid flow problems have not been adequately studied. CFD software are commonly used nowadays (Jiang *et al.,* 2017) to solve such nozzle problems. Fluid flow, chemical reactions and heat transfer problems, which are difficult and time consuming to run experimentally, can be easily be solved with these CFD simulation methods. CFD software packages have user friendly interface and allow the user to test many parameters, which would be difficult to do in real world. Recent advances in computer hardware make it easy to solve many complex industrial and academic problems related to fluid flow with more accuracy and low computation time.

With all above mentioned reasons, it is necessary to study the spraying behavior for reducing spray losses. In particular, it is important to understand how the fluid jet behaves at different pressures as it is directly linked to spray losses. In this paper, we examine the velocity distribution of agricultural spraying nozzles by using numerical simulation (commercial software ANSYS 16.0, Fluent) and validate the results with jet velocity study by a PIV experiment. Velocity distribution is one of the key factors linked with spray drift. The PIV technique is a non-intrusive laser optical measurement technique used to obtain instantaneous velocity vectors in a cross-section of gas or liquid flows. The details of the PIV experimental method can be seen in our previous work (Nadeem *et al.,* 2018). Two outcomes of this work are: i) to provide better insight into jet behavior in terms of velocity, which will identify the weak areas of spray, and where there is the maximum probability of drift prone particles; ii) to open a new horizon in spraying system research of flat fan nozzle, which will not only decrease the experimental cost but also reduce the labor and time for nozzle analysis. The overall gain of this work can lead to a reliable dataset that will be used to optimize the design of sprayer nozzle for less spraying losses. The flowchart in Fig. 1 represents all different steps involved in this study.

MATERIALS AND METHODS

Mathematical background for Computational Fluids Dynamics (CFD):

***Reynolds number*:** In most of fluid flow problems, the first and foremost step is to find out the nature of flow, whether it is laminar or turbulent. Before selecting the appropriate model for simulation, the Reynolds numbers (Re) at different pressures was calculated using Equation (1) and presented in Table 1.

$$Re = Vd/\mu \quad (1)$$

Where v: Jet velocity at inlet (m/s), d: diameter of orifice (m), µ: Kinematic viscosity (m^2/s)

Table 1. Relationship between pressure and Reynolds number.

P (kPa)	V (m/s)	Re
25	6.837	10215.73
50	9.950	14865.66
75	12.025	17965.60
100	15.208	22721.21
125	16.504	24658.67
150	17.330	25891.61
175	18.509	27652.94
200	20.324	303650.40

P= Pressure at the tip of nozzle (kPa), V= Jet velocity at the tip of nozzle (m/s) using PIV

The values of Reynolds numbers (Table 1) were very high so the flow conditions were considered as turbulent flow (Sinha *et al.*, 2015; Iqbal *et al.*, 2005). To deal with turbulent flow many researchers used the *k*-ε modeling approach (Altimira *et al.*, 2009; Jonsen, 1992; Menter *et al., 2003;* Shirani *et al., 2006*; Shih *et al.*, 1995; Tiwari *et al.*, 2014).

Turbulence regime: The standard *k*-epsilon model was used for the simulation of turbulent flow through the spray nozzle. This model is composed of two parameters which model the turbulence kinetic energy (*k*) and the dissipation rate (ε). The standard *k*-epsilon model is based on the assumption that the flow is in fully turbulent conditions while neglecting the viscosity. This model has been found to be reliable, accurate and simple with very fast convergence and is widely used to study flow problems (Jiang *et al.*, 2017; Sinha *et al.*, 2015; Tiwari *et al.*, 2014; Altimira *et al.*, 2009; Najjar *et al.*, 1995).

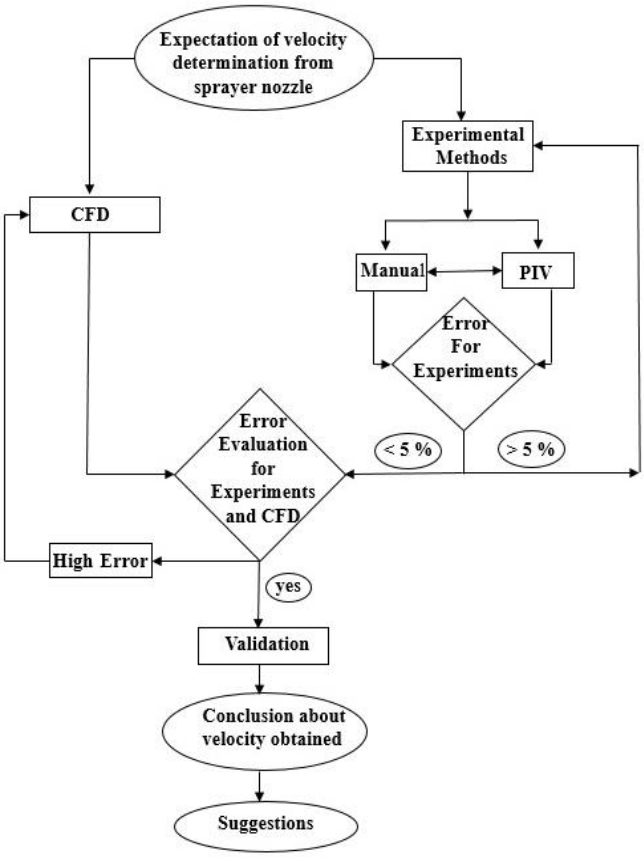

Figure 1. Schematic diagram of analysis for spray nozzle measurement.

Governing Equations for k-epsilon model

$$\frac{\partial U_{i,k}}{\partial X_i} = 0 \quad (2)$$

$$\frac{\partial}{\partial t}(\rho_k U_{i,k}) + \frac{\partial}{\partial X_i}(\rho_k U_{i,k} U_{j,k}) = -\frac{\partial p_k}{\partial X_i} + \frac{\partial}{\partial X_i}\left[U_k\left(\frac{\partial U_{i,k}}{\partial X_j}\right)\right] \quad (3)$$

$$[U_i] = 0$$

$$\left[\left(\tau_{ij} \cdot n_i\right) \cdot n_i + p\right] = \sigma \cdot k \quad (4)$$

$$\left[\left(\tau_{ij} \cdot n_i\right) \cdot t_j\right] = 0 \quad (5)$$

Where; u_i: Velocity component in corresponding direction (m/s), ρ: density of fluid (kg/m^3), and k: turbulence kinetic energy.

***Volume of fluid (VOF)*:** There are several methods listed in the literature to simulate the multiphase flow described by the conservation of mass and conservation of flow equations. Normally these methods are classified into two major categories based on their flow domain and method of discretization (Lakehal *et al.*, 2002).

In the first category, each phase (fluid) is considered as a deformable flow domain and solutions can be discretized to solve the mass and momentum equations at each time step (Ryskin and Leal, 1984). Interphases between two phases (water and air) would be the straightforward boundary conditions of the different phase domains. These models used in this category encounter difficulties when dealing with high-distorted domains. In the second category, the domain of flow is considered fixed. An additional processor is used to define the interface between two different phases (water and air). A system of differential equations for fluid (mixture) is used to solve the fixed domain. The whole domain is modeled in such a way that different phases allow the spatial variation in fluid properties such as density and viscosity, and conditions of jumps are modeled separately. To identify the interface, there are two different methods under this category: the front tracking method and the front capturing method

In the front tracking method, the particles of moving fluids are used to identify the interface (Harlow and Welch, 1965). In the front capturing method, the mark function (using different colors) is utilized to identify the interface. To solve this mark function, additional differential equations are needed to be solved to locate the interface. VOF is one of the famous front capturing methods (Hirt and Nichols, 1981; Gueyffier *et al.*, 1999). VOF was used to track the air and water phase during the simulation of sprayer nozzle. VOF method defined the fraction of water and air (Albadawi *et al.*, 2013; Lv *et al.*, 2011; Lakdawala *et al.*, 2014). The 0 value of variable α defines the availability of air while 1 represents water. To define the water and air both in one grid the VOF method assigned the value in-between 0 and 1 (Altimira *et al.*, 2009; Cock *et al.*, 2014).

Governing equations for VOF method

$$\frac{\partial \alpha}{\partial t} + \frac{\partial}{\partial X_i}(\alpha u_i) = 0 \quad (6)$$

$$\rho = \alpha\rho_1 + (1-\alpha)\rho_g \quad (7)$$

$$u = \alpha u_1 + (1-\alpha)u_g \quad (8)$$

$$\frac{\partial \rho}{\partial t} + \frac{\partial \rho u_1}{\partial X_i}\left[U_k\left(\frac{\partial U_{i,k}}{\partial X_j}\right)\right] \quad (9)$$

Where α: marker function (0 or 1), u: particle velocity (m/s), ρ : density of fluid (kg/m^3)

Jet velocity calculation from the experimental discharge data

Iqbal *et al.* (2005) reported a formula to calculate the jet velocity at the tip of nozzle with known diameter.

Volumetric flow rate:

$Q = V_j\, C_a\, A$ (10)

Where Q = flow rate or discharge (m^3/s), V_j = Jet velocity (m/s), C_a = Area coefficient, and A=Nozzle surface area (m^2).

Jet velocity:

$Vj = C_v\, (2\, \Delta p\, /\rho)^n$ (11)

Where; Vj = Jet velocity (m/s), C_v = velocity coefficient, Δp = Total pressure drop (Pa), ρ=Liquid density (kg/ m^3), n = 0.5 for turbulence flow, C_d = Coefficient of discharge.

Substituting the value of "V_j" from equation (10) into equation (11) gives

$Q = C_v\, (2\, \Delta\, p\, /\rho)^{0.5}\, C_a\, A$ (12)

Let $C_v\, C_a = C_d$ then $Q = C_d\, (2\, \Delta\, p\, /\rho)^{0.5}\, A$

Where; $(2\, \Delta p\, /\rho)^{0.5} = (2gh)^{0.5} = V_j$

So, equation (4) becomes $Q = C_d\, V_j\, A$

$V_j = Q\, /\, C_d\, A$ (13)

Equation (13) was used to calculate the average jet velocity. For this equation, we need Q, C_d and A. For measuring the value of Q, a 1-liter graduated beaker was used to collect the volume of water for one minute and discharge was calculated by as volume/time while the nozzle was operated at eight different pressures. This method was repeated three times and the average discharge or flow rate of the nozzle was calculated as presented in Table 2.

Table 2. Effect of pressure on discharge.

Pressure (kPa)	$(P)^{1/2}$	Q (m^3/sec)
25	5.00	4.830E-06
50	7.07	7.033E-06
75	8.66	8.500E-06
100	10.00	10.750E-06
125	11.18	1.166E-05
150	12.25	1.225E-05
175	13.23	1.308E-05
200	14.14	1.436E-05

** P= Pressure at the tip of nozzle (kPa), Q= flow rate (m^3/s) measured manually*

The value of C_d, was calculated as the slope of the line between Q and $\sqrt{p}$.

$Q = Cd\sqrt{(2\Delta\, p\, /\rho)}\ A$

$Q = Cd\sqrt{(2\, /\rho)}\ A\sqrt{\Delta\, p}$

$Q/\sqrt{\Delta\, p}\ = Cd\sqrt{(2\, /\rho)}$ A = slope of line

So, $Cd = Q/\sqrt{\Delta\, p}\ /\ \sqrt{(2\, /\rho)}$ A (14)

Simulation and Experimental setups

***CFD simulation by the commercial software ANSYS*:** Modelling turbulence flow using *k*-epsilon and VOF approaches simultaneously for sprayer nozzle at different pressures is a very complex task due to the many factors involved. To deal with this problem, the software ANSYS 16.0 (Fluent) was used. Many CFD packages are available with comprehensive and user-friendly interface for both pre-processing and post-processing processes (Sinha *et al.*, 2015).

Geometry: 2-D model of sprayer nozzle was created by using the design module available in ANSYS 16.0. The model included key parts of the nozzle and the environment which is comprised of water and air (Fig. 2). The inlet area was selected as water, while the outlet area was selected as air at STP (Standard temperature and pressure) condition (Fig. 2).

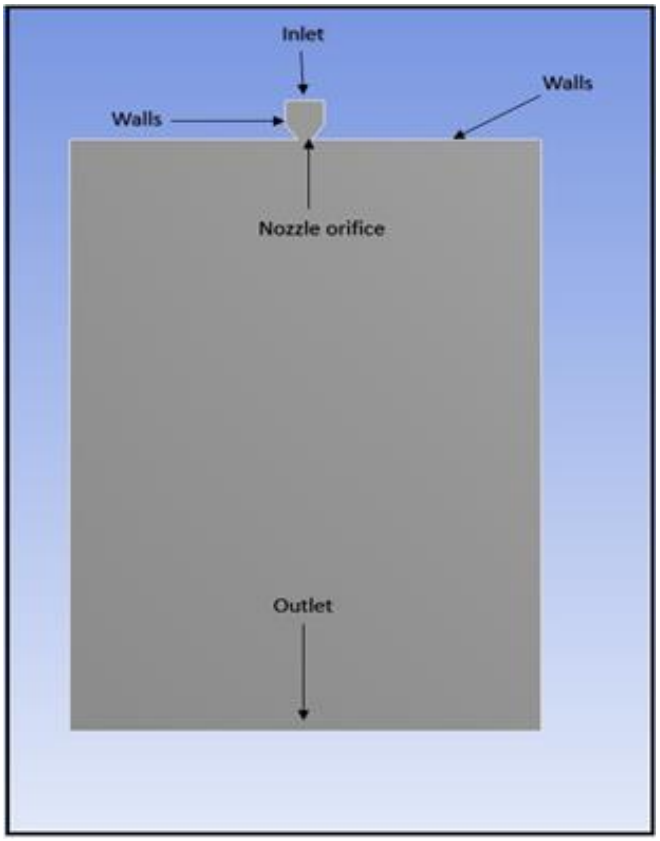

Figure 2. Geometry of nozzle and flow domain.

***Meshing*:** Three different meshes were tested for this study: coarse, fine and very fine mesh. A mesh sensitive analysis was conducted to check the influence of mesh on computational results. Mesh with 56741 nodes and 56243 elements (Fig. 3a) was considered the best option for this study because there was no significant difference between very fine and fine mesh except computational time while the coarse mesh with 14380 nodes and 14127 elements were not considered for further calculations due to significantly worse simulation results. For the fine and very fine meshes, the results indicated that the results were similar and independent of mesh size. The fine

mesh was selected for further simulation because it took less computation time without changing the results.

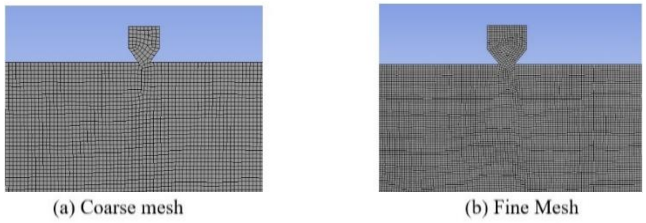

Figure 3. Mesh analysis.

Boundary conditions: The following boundary conditions for CFD simulations were used. The nozzles portion of geometry was selected as water fluid (density 1000 kg/m^3) with different pressure conditions. The remaining geometry portion after the nozzle tip was considered as air at 100 kPa. At the inlet, the pressure is varied between 25 kPa to 200 kPa for both the numerical simulation and experimental setup.

Method of PIV to experiment Jet velocity measurements:

PIV experimental setup: To validate the CFD modeling results the experimental setup was used to simulate the nozzle at different pressures (25, 50, 75, 100, 125, 150, 175, 200 kPa). A schematic diagram for a PIV system is shown in Figure 4a. The standard PIV (Two-dimensional PIV system from LPU 550, Dantec Dynamics (Fig. 4b) was used to take the laser-illuminated images for the acquisition of spray behavior (velocity of jet). Details of all parameters were kept the same as in our previous work (Nadeem *et al.*, 2018).

The main objective of PIV imaging was to measure the particle displacement and time so that velocity of individual particles could be calculated. In the case of submerged flow, seeded particles (having same density of fluid used for simulation) were used to mimic the flow. The displacement of these particles can be calculated by using post-processing tools available in Dynamic Studio (Computer based software). In the case of nozzle flow, water was coming out into the air directly, droplets of water were hence illuminated by laser beam and the CCD cameras were used to capture these images (Fig.7a).

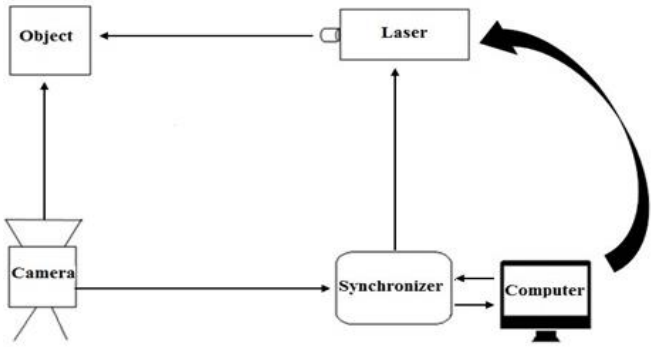

Figure 4a. Schematic diagram of Particle Image Velocimetry (PIV) system (Nadeem *et al.*, 2018).

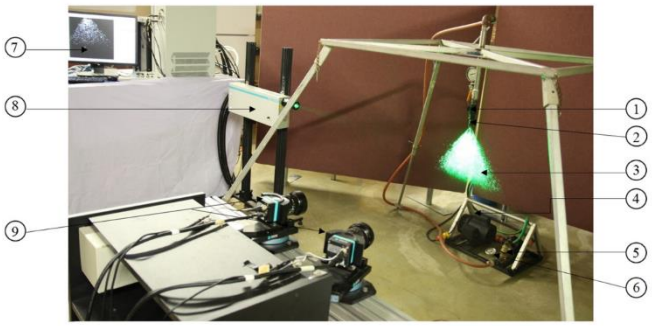

A= Prototype of spray nozzles B= Operational components of PIV 1. Pressure gauge, 2. Flow control valve 3. Nozzle assembly 4. Spray sheet with laser 5. Electric motor, 6. Suction and bypass pipe 7. Pressure control valve, 8. Pressure gauge 9. Synchronizer 10. Computer, 11. Laser controller 12. YLF laser 13. CCD cameras.

Figure 4b. PIV system and prototype of sprayer nozzle (Nadeem *et al.*, 2018).

***Post processing of acquired images*:** Choosing optimal recording parameters and setting the proper parameters for processing require experience, especially the section of interrogative area (IA), balancing robustness, precision and accuracy of flow fields. The goal of the image interrogation was to measure the displacement between different pattern images with high accuracy. For this purpose, the images were divided into small areas called "interrogation area" (normally 16 x 16 and maximum 128 x 128 pixels). Then adaptive correlation was used to determine the displacement value for each small IA area. There are no set rules and optimal conditions for different types of flow due to variable seeding density, variable quality of images and flow conditions (Theunissen *et al.*, 2006; Dantec Dynamics, 2013). The adaptive correlation was considered as automatic adaptive method to calculate the velocity vector by adjusting the shape and size of IA based on the flow adaptivity (flow gradient) and signal adaptivity (signal quality). Such type of automatic system leads to more accuracy and spatial resolution especially in the high gradient regions. (Theunissen *et al.*, 2006).

Therefore, the adaptive correlation method, a very user-friendly technique, was chosen to calculate the velocity vectors to improve the spatial resolution, speed, and accuracy. The second main advantage of this technique is that it controls the brightness, image focus and time step (Dantec Dynamics, 2013). Our results using the adaptive correlation showed statistically matching between two images, and the location of highest peak value of displacement was measured as average particle displacement, considered as velocity vector.

RESULTS AND DISCUSSION

Based on our framework (Fig.1), the results obtained in each step will be discussed. The jet velocity was measured at the tip of sprayer nozzle by using: a) the experimental measurement including PIV and manual methods (right branch of Fig.1); and b) numerical simulation by CFD (left branch of Fig. 1).

***Tip velocity measurement*:** In the CFD numerical simulation, we used ANSYS 16 Fluent software to simulate the nozzle at eight different pressures (25, 50, 75, 100, 125, 150, 175, 200 kPa) and results of tip velocity were tabulated in Table 3 (column 5).

Table 3. Comparison of jet velocity measured with experimental data and simulation.

P (kPa)	$(P)^{1/2}$	Q (m^3/sec)	Simulation "V" (m/s)	PIV "V" (m/s)	Manual "V" (m/s)
25	5.00	4.83E-06	6.64	6.8933	6.84
50	7.07	7.03E-06	9.43	8.6371	9.95
75	8.66	8.50E-06	11.06	11.5245	12.03
100	10.00	10.75E-06	13.40	13.4137	15.21
125	11.18	1.17E-05	14.90	15.5234	16.50
150	12.25	1.22E-05	16.40	17.6296	17.33
175	13.23	1.31E-05	17.70	18.4578	18.51
200	14.14	1.44E-05	19.45	20.1845	20.32

** P= Pressure at the tip of nozzle (kPa), Q= flow rate (m^3/s), V= Jet velocity (m/s)*

After obtaining this CFD tip velocity, the experimental techniques, including PIV and manual methods were used to find out the tip velocity for this nozzle. The PIV method was used to capture the real-time images by using the experimental setup mentioned in the previous section. These images were processed to find out the tip velocity and tabulated in Table 3 (column 6). Beside the PIV method, a manual measurement was also used to quantify the tip velocity. For this approach, Equations (10) to (14) were used. Equation 13 was used to calculate the velocity with Q, C_d, and A as inputs. The values Q were measured using the volumetric method and are presented in column 4 of Table 3. A was calculated based of the nozzle diameter as shown below.

Diameter of nozzle: D = 1.5 mm

Radius of nozzle: r = 0.00075 m

Surface area of nozzle: $\pi r^2 = 1.76 \times 10^{-6}\ m^2$

For C_d, the slope of the line from Fig. 5 was used.

$$Q/\sqrt{\Delta p} = 1 \times 10^{-6}$$

According to equation (14), the C_d was calculated as

$$1 \times 10^{-6} / \sqrt{1000} = C_d \times (1.76 \times 10^{-6}) \times (1.4121 \times 0.03162)$$

$$C_d = 0.316 \times 10^{-6} / 0.07858 \times 10^{-6}$$

$$C_d = 0.40$$

Knowing the value of C_d, Q, and A, the jet velocity V can be obtained from Equation (13) and is reported in column 7 of Table 3.

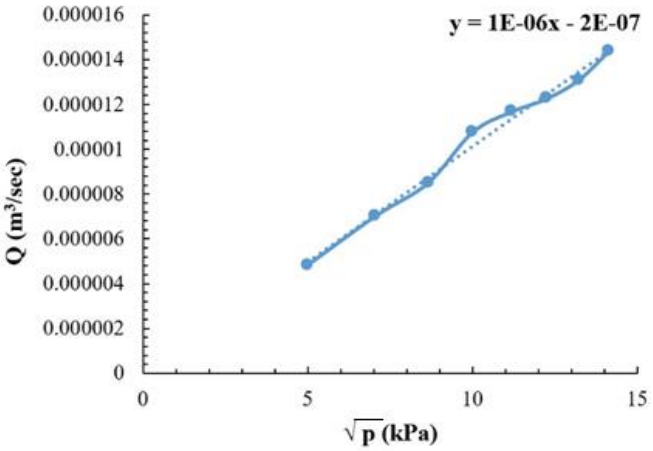

Figure 5. Coefficient of discharge for extended flat fan nozzle.

***Error estimation and validation*:** The results of these three methods (Table 3) showed that the tip velocity of sprayer nozzle was increasing from 25 kPa to 200 kPa by using CFD numerical simulation and the same trend was observed with the PIV and manual experimental methods. The tip velocity values obtained by these three methods are very close to each other within ± 1% error. At a pressure of 25 kPa, the tip velocities are very close to each other within ± 0.5% error. However, the error is less than 5% in most cases when comparing CFD numerical simulation with PIV and manual experimental methods (Table 3). When the pressure increases these measured values start to diverge, not as homogenous as with the 25 kPa case. This could be explained by the fact that higher pressure causes high turbulent regime governed by high Reynolds number (Table 1). Figure 6 presents the relationships of nozzle pressure (kPa) versus jet velocity (m/s) obtained by the three different methods: CFD, PIV and manual measurements.

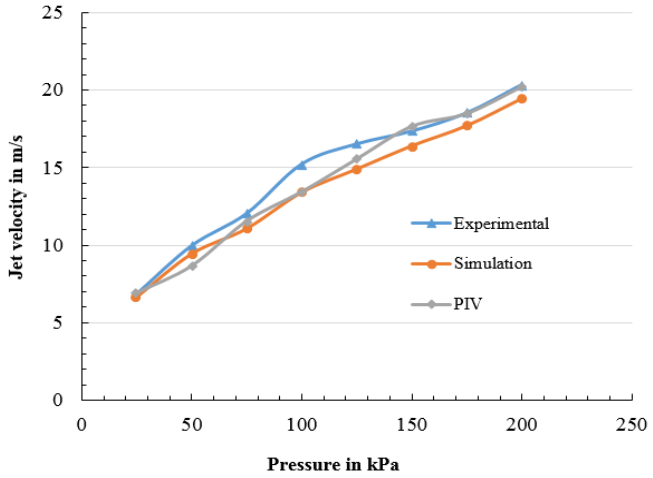

Figure 6. Comparison of jet velocity.

It is noticed that the numerical simulation velocity by CFD mostly overlapped the manual and PIV experimental results. There was however a mismatch between the CFD numerical and manual results at the pressure of 100 kPa, which can be due to the human error during operation.

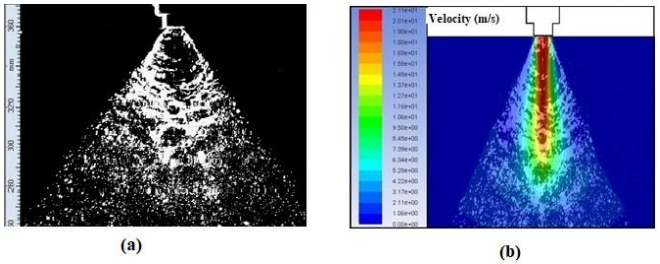

Figure 7. PIV image captured at 200 kPa (a), Overlapping of PIV and CFD images at 200 kPa.

The results overlapped at high pressure (200 kPa) (Fig. 7). Figure 7 illustrates the flow pattern obtained through the PIV. ***Behavior of spray velocity under nozzle tip at different positions*:** Figure 8 shows the velocity distribution at different points under the sprayer nozzle at 200 kPa pressure (precisely, at 10, 20, 30, 40 and 50 mm as shown in Figure 8). The tip velocity changes from 20.02 m/s to 12.00 m/s along the central line of flow. It was observed that there was a deceleration of velocity from top to bottom along the central line due the impact of air.

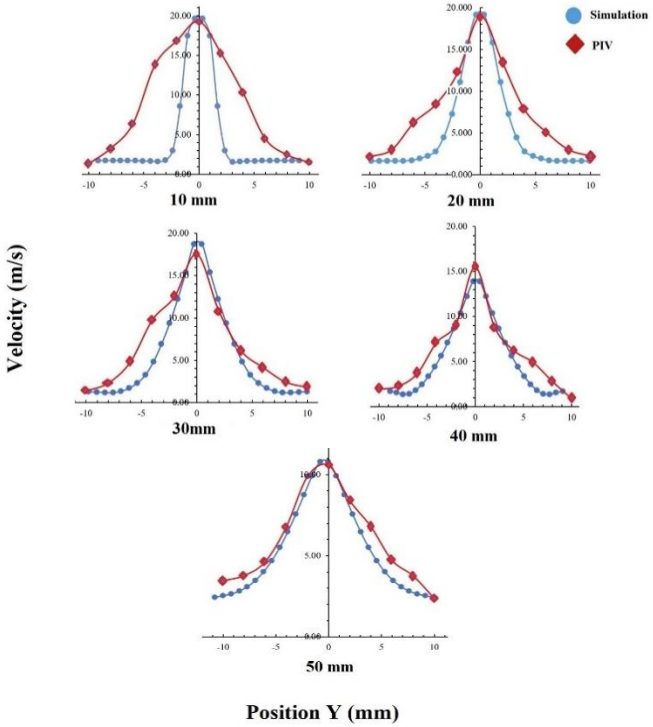

Figure 8. Velocity profiles at different points under the nozzle: numerical simulation and PIV.

At the 10 mm position, PIV and CFD numerical simulation results did not overlap, it may be due to the abrupt entrance of the air at tip points. The entering air at this point changed the velocity in the case of PIV. As water moved down, the velocity profiles overlapped better. The velocity distribution was also verified through PIV images at five different positions (10, 20, 30, 40 and 50 mm) under the sprayer nozzle. All velocity vectors data were plotted against their frequencies (Fig. 9) and showed that the velocity data followed the normal distribution with mean and median values of 8.84 and 9.5 respectively. The mean and median values were very close to each other, which showed that the spray particles were uniformly distributed. When the mean value approaches the median of a distribution in an ideal scenario, it means that the distribution (velocity) is perfectly symmetrical. However, this perfect scenario may not happen due to the asymmetrical laser source (the laser beam just coming from one side), enlightened situation for each PIV image was not the same etc. Hence, our graph in Figure 9 is not a perfectly symmetrical normal distribution.

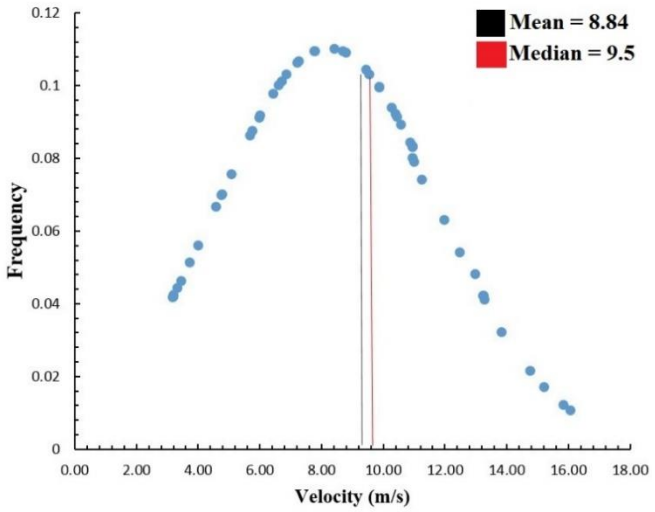

Figure 9. Velocity distribution under the sprayer nozzle at 200 kPa pressure.

***Remark on the velocity values measured*:** At different positions, the numerical simulation and PIV methods give similar results. Fig. 8 shows the overlapping of velocity of these two methods. It can be also seen from this figure that the velocity of spray is decreasing in both PIV and numerical simulation cases while being at lower positions of the nozzle and the width of jet is spreading. The PIV and CFD numerical simulation given are in good agreement despite some mismatching points.

The PIV method is a reliable option for measuring the jet velocity and very helpful to map the velocity distribution under the nozzle. This method incorporates all the fluctuation of pressure and the changing behavior of the air around the nozzle jet.

The numerical simulation is also a reliable method for mapping the velocity distribution under nozzle. But the velocity profile obtained through numerical simulation is not completely overlapping with PIV velocity profile near nozzle tip (10 mm) (Fig. 8). The main reason of this mismatching could be the pressure drop at tip of nozzle due to very high velocity and the surrounding air mixing with the water jet. The mixing of air at this point could result in high turbulence. The second main cause of this variation could be the slight change in pressure due to pump fluctuation.

***Different applications from the findings of this study*:**

1. The present study confirmed again that during spraying from through a nozzle, maximum velocity occurs in the center of the spray sheet which has the maximum probability to hit the right target (on plant surface). At this high velocity (20-16 m/s), there are less chances of droplet to escape from the spray sheet. The other good aspect of this part is that if we need to apply the spot specific application as in case of early stages of many row crops then proper volume of chemical could be applied by using only one nozzle per row. This study showed with a more precise and qualitative way that the outer layer of spray sheet has minimum velocity. This part of spray is very sensitive to drift. Due to low velocity of spray sheet, the droplets could blow off target and could contaminate the air by suspending in the air or can cause contamination of off field soils. To avoid this situation, we recommend to adjust the boom height as low as possible in early stage of crop, while allowing the overlapping of spray sheets when crop canopy is fully developed.
2. The results of this study could be very useful for the uniform application of edible coating on fruits (an emerging food science topic) (Andrade *et al*., 2012) uniform protective coating for meat (Spraying system, 2013) fire sprinkler (Husted *et al.,* 2009), sprinkler and drip irrigation (Yunkai *et al.,* 2008) and to study the behaviour of nozzle injectors (Vimal and Gupta, 2015).
3. The results of simulation and experimental validation of jet velocity were used to predict the jet velocity behavior at high pressure. The jet velocity has a parabolic trend as shown in Fig. 10. The predicted pressure velocity relationship (Fig. 10) could be very usefully for many industrial applications (fruit coating, car painting, high-pressure fuel injection, tablet coating etc.). According to this predicted jet velocity (Fig. 10) the velocity of spray jet had increasing trend with increase in pressure. However, the increasing pressure also had impact on decreasing the droplet size. For better penetration of spay we need to find an optimal pressure where we will attain the optimal velocity (high velocity will lead to runoff after slipping from the leaves, and low velocity will lead to more drift) with optimal droplet size because increasing the pressure will increase the risk of drift by making mist of spray in agricultural application. At low pressure, the velocity of jet will be less and spray sheet

will be more drift prone.

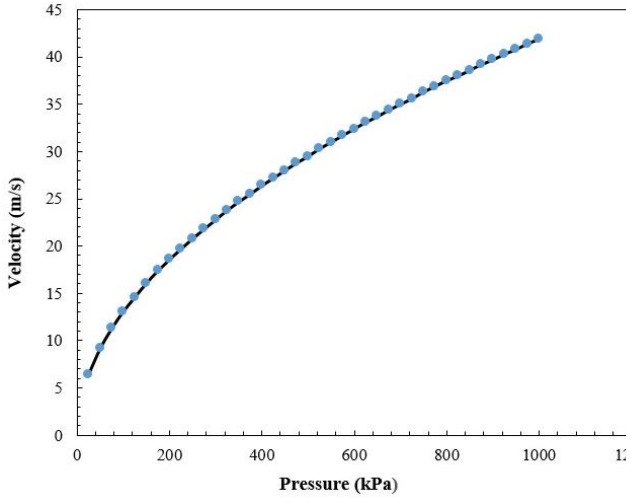

Figure 10. Jet velocity prediction at high pressure.

Selection of proper pressure will lead to the less spray losses and uniform distribution. There is a need of comprehensive research on spray drift to consider all the possible factors, which are influencing the spray drift.

***Conclusion*:** The results of this study showed that the spray sheet had maximum velocity at its centre. The particles present in the central region of spray sheet will have maximum kinetic energy and that region have the maximum probability to hit the right target. The spray particles present in the surroundings of the central part had the less velocity that would lead to minimum kinetic energy. This part of spray would be the more sensitive part of spray. There are maximum chances of off target drift only on these parts. Due to low kinetic energy, these particles can move away from the targets surfaces easily even with very low wind velocity.

Both PIV and ANSYS 16.0 simulation methods were proven as appropriate tools to investigate the distribution pattern of flat fan nozzles and can be considered as reliable and cost-effective research methods for such type of complex nozzles flow. Although the research result has more or less a known common sense of spraying nozzles, the performance of the study by using PIV technique confirms quantitatively some accurate and precise values of droplet velocity, validated by simulation, is our main finding here as no previous work was focusing on it.

The overall results of this study showed that the edges of spray sheet and spray away from the tip of nozzle had low velocity and these parts are at high risk for drift. The spray from these parts have maximum probability to move away from the target. This off-target spray could cause the soil and water contamination. To reduce this off-target spray, there is a need of comprehensive research on spray drift to consider all the possible factors, which are influencing the spray drift. The results of this study can be very useful for the uniform application of edible coating on fruits (an emerging food science topic), uniform protective coating for meat, fire sprinkler, sprinkler irrigation and to the study of nozzle injectors.

***Acknowledgements*:** This work was supported by the Canada Foundation for Innovation (CFI) Grant No 31188, Nova Scotia Research and Innovation Trust (NSRIT) and Natural Sciences and Engineering Research Council of Canada NSERC RGPIN 03796 of TNQ. MN wants to acknowledge the support from University of Agriculture Faisalabad (Pakistan).

REFERENCES

Altimira, M., A. Rivas, G.S. Larraona, R. Anton and J.C. Ramos. 2009. Characterization of fan spray atomizers through numerical simulation. Int. J. Heat Fluid Fl. 30:339-355.

Albadawi, A., D.B. Donoghue and A.J. Robinson. 2013. Influence of surface tension implementation in volume of fluid and coupled volume of fluid with level set methods for bubble growth and detachment. Int. J. Multiphase Flow 53:11-28.

American Society of Agricultural and Biological Engineers. 2010. Spray nozzle classification by droplet spectra. Standard Technical Note - S572 Chart. ASABE, Saint Joseph, Missouri, United States of America.

Andrade, D.R., O. Skurtys and F.A. Osorio. 2012. Atomizing spray systems for application of edible coatings. Compr. Rev. Food Sci. Food Saf. 11:323-337.

Bird, S.L., D.M. Esterly and S.G. Perry. 1996. Off-target deposition of pesticides from agricultural aerial spray application. J. Environ. Qual. 25:1095-1104.

Carlsen, S.C.K., N.H. Spliid and B. Svensmark. 2006. Drift of 10 herbicides after tractor spray application: 2. Primary drift (droplet drift). Chemosphere 64:778-786.

Chaudhary, K. and T. Maxworthy. 1980. The nonlinear capillary instability of a liquid jet. Part 2. Experiments on jet behavior before droplet formation. J. Fluid Mech. 96:275-286.

Cock, N.D., M. Massinon, N.B.C. Mercatoris and F. Lebeau. 2014. Numerical modelling of mirror nozzle flow. In: American Society of Agricultural and Biological Engineer (ASABE); Montreal, Quebec, Canada; pp.1-9.

Derksen, R.C., H. Zhu, H.E. Ozkan, R. B. Hammond, A.E. Dorrance and A.L. Spongberg. 2008. Determining the influence of spray quality, nozzle type, spray volume, and air-assisted application strategies on deposition of pesticides in soybean canopy. Trans. ASABE 51:1529-1537.

Dantec Dynamics. 2013. Dynamic Studio User Guide, 2nd Ed. Tonsbakken 18, DK-2740 Skovlunde, Denmark.

Etheridge, R.E., A.R. Womac and T.C. Mueller. 1999. Characterization of the spray droplet spectra and patterns of four venture-type drift reduction nozzles. Weed Technol. 13:765-770.

Farooq, M., R. Balachandar, D. Wulfsohn and T.M. Wolf. 2001. Agricultural sprays in cross flow and drift. J. Agric. Eng. Res. 78:347-358.

Gueyffier, D., J. Li, A. Nadim, R. Scardovelli and S. Zaleski. 1999. Volume of Fluid interface tracking with smoothed surface stress methods for three-dimensional flows. J. Comput. Phys. 152:423-456.

Harlow, F.H. and E. Welch. 1965. Numerical calculation of time-dependent viscous incompressible flow of fluids with free surface. Phys. Fluids 8:2182-2192.

Hirt, C.W. and B.D. Nichols. 1981. Volume of Fluid (VOF) method for the dynamics of free boundaries. J. Comput. Phys. 39:201-225.

Homma, S., J. Koga, S. Matsumoto, M. Song and G. Tryggvason. 2006. Breakup mode of an axi-symmetric liquid jet injected into another immiscible liquid. Chem. Eng. Sci. 61:3986-3996.

Husted, B.P., P. Petersson, I. Lund and G. Holmstedt. 2009. Comparison of PIV and PDA droplet velocity measurement techniques on two high-pressure water mist nozzles. Fire Saf. J. 44:1030-1045.

Iqbal, M., M. Ahmad and M. Younis. 2005. Effect of Reynold's number on droplet size of hollow cone nozzle of environment friendly university boom sprayer. Pak. J. Agri. Sci. 42:106-111.

Jiang, Y., H. Li, Q. Xiang and C. Chen. 2017. Comparison of PIV experiment and numerical simulation on the velocity distribution of intermediate pressure jets with different nozzle parameters. Irrig. Drain. 66:510-519.

Jonsen, T. 1992. Simulation and modeling of turbulence incompressible flows. Ph.D. diss., Dept. of Comput. Engg., Swiss Feder. Inst. of Technol., Lausanne, Switzerland.

Piggott, S. and G.A. Matthews. 1999. Air induction nozzles: A solution to spray drift? Intl. Pest Cont. 41:24-28.

Lakdawala, A.M., V.H. Gada and A. Sharma. 2014. A dual grid level set method based study of interface-dynamics for a liquid jet injected upwards into another liquid. Int. J. Multiphas Flow 59:206-220.

Lakehal, D., M. Meier and M. Fulgosi. 2002. Interface tracking towards the direct simulation of heat and mass transfer in multiphase flows. Int. J. Heat Fluid Fl. 23:242-257.

Lin, S.P. and R.D. Reitz. 1998. Drop and spray formation from a liquid jet. Ann. Rev. Fluid Mech. 30:85–105.

Lv, X., Q.P. Zou and D. Reeve. 2011. Numerical simulation of overflow at vertical weirs using a hybrid level set/VOF method. Adv. Water Res. 34:1320-1334.

Menter, F.R., M. Kuntz and R. Langtry. 2003. Ten years of experience with the SST turbulence model. In: Proceeding of the fourth international symposium on turbulence, heat mass transfer, Antalya, Turkey; pp.625-632.

Miller, P.C.H. and M.C. Butler Ellis. 1997. A review of spray generation, delivery to the target, and how adjuvants influence the process. Plant Prot. Quart. 12:33-38.

Nadeem, M., Y.K. Chang, U. Venkatadri, C. Diallo, P. Havard and T. Nguyen-Quang. 2018. Water quantification from sprayer nozzle by using particle image velocimetry (PIV) versus imaging processing technique. Pak. J. Agri. Sci. 55:203-210.

Najjar, F.M., B.G. Thomas and E.H. Donald. 1995. Turbulent flow simulations in bifurcated nozzles: effects of design and casting operation. Metall. Trans. B. 26:749-765.

Nuyttens, D., M.D. Schampheleire, K. Baetens and B. Sonck. 2007. The influence of operator-controlled variables on spray drift from field crop sprayers. Trans. ASABE 50:1129-1140.

Nuyttens, D., M.D. Schampheleire, P. Verboven, E. Brusselman and D. Dekeyser. 2009. Droplet size and velocity characteristics of agricultural sprays. Trans. ASABE 52:1471-1480.

Ozkan, H.E., H. Miralles, H. Zhu, D.R. Reichard and R.D. Fox. 1997. Shields to reduce spray drift. J. Agric. Eng. Res. 67:311-322.

Ozkan, H.E. 1998. Effects of major variables on drift distances of spray droplets. Fact Sheet AEX 525-98. Columbus, Ohio State University Extension, United State of America.

Ryskin, G. and L.G. Leal. 1984. Numerical solution of free-boundary problems in fluid mechanics. Part 2. Buoyancy-driven motion of a gas bubble through a quiescent liquid. J. Fluid Mech. 148:19-35.

Shih, T.H., W.W. Liou, A. Shabbir, Z. Yang and J. Zhu. 1995. A new k-e eddy-viscosity model for high Reynolds number turbulent flows- model development and validation. Comput. Fluid 24:227-238.

Shirani, E., A. Jafari and N. Ashgriz. 2006. Turbulence models for flows with free surfaces and interfaces. AIAA J. 44:1454-1462.

Sinha, A., B. Sridhar and G. Shivasubramanian. 2015. A numerical study on dynamics of spray jets. Ind. A. Sci. 40:787-802.

Smith, D.B., S.D. Askew, W.H. Morris and M. Boyette. 2000. Droplet size and leaf morphology effects on pesticide spray deposition. Trans. ASAE 43:255-259.

Spraying system. 2013. A guide to spray technology for food processing, solutions for coating, cleaning, drying, food safety & more. Available online with updates at https://spray-nozzles.co.za/wp-content/uploads/2014/06/B524D_Food_Processing.pdf

Taylor, J.J. and J.W. Hoyt. 1977. Waves on water jet. J. Fluid Mech. 83:119-127.

Theunissen, R., F. Scarano and M.L. Riethmuller. 2007. An adaptive sampling and windowing interrogation method in PIV. Meas. Sci. Technol. 18:275-287.

Theunissen, R., F.F.J. Schrijer, F. Scarano and M.L. Riethmuller. 2006. Application of adaptive PIV interrogation in a hypersonic flow. In: Proceedings of the 13th international symposium on applications of laser techniques to fluid mechanics, Lisbon, Portugal; pp.26-29.

Tiwari, A.K., P. Ghosh, J. Sarkar, H. Dahiya and J. Parekh. 2014. Numerical investigation of heat transfer and fluid flow in plate heat exchanger using nano-fluids. Int. J. Therm. Sci. 85:93-103.

Vimal, K.P. and S. Gupta. 2015. Study of nozzle injector performance using CFD. Int. J. Rec. Ad. Mech. Engg. 4:153-160.

Yarpuz, N. and A.M. Bozdogan. 2009. Comparison of field and model percentage drift using different types of hydraulic nozzles in pesticide applications. Int. J. Environ. Sci. Tech. 6:191-196.

Yunkai L., P. Yang, T. Xu, S. Ren, X. Lin, R. Wei and H. Xu. 2008. CFD and digital particle tracking to assess flow characteristics in the labyrinth flow path of a drip irrigation emitter. Irrig. Sci. 26:427-438.